

rung der Fußrollenanstellung konnte der Erstarrungsfortschritt vergleichmässigt und die Produktqualität eindeutig verbessert werden.

Oberflächentemperaturmessung:

Durch den Einsatz von Pyrometern mit Lichtleitertechnologie konnten erstmalig periodische Vorgänge während der Erstarrung ermittelt werden. Eine Auswirkung dieser periodischen Vorgänge auf die Produktqualität konnte nicht nachgewiesen werden. Um die Erstarrungsvorgänge zu vergleichmässigen, wurden nachstehende Maßnahmen umgesetzt:

- Vermeidung des kritischen Geschwindigkeitsbereiches
- Verbesserung der Regelbarkeit der Sekundärkühlung bei geringen Wassermengen

Reibkraftmessung:

Durch die Reibkraftmessung konnte der Nachweis des Kokillenalters auf die Reibarbeit und damit auf den Spannungsaufbau in der Strangschale erbracht werden.

7. Ausblick

Nachdem die einzelnen Messmethoden erste vielversprechende Ergebnisse geliefert haben, sind nachstehende Aktivitäten geplant:

- Kombination der Messsysteme zur besseren Beurteilung von periodischen Vorgängen bzw. instationären Zuständen (Änderung der Gießgeschwindigkeit, Gießspiegelschwankungen)
- Labortests zur Überprüfung von Prozessparametern (z. B. Wärmestromdichte) und Ermittlung von Werkstoffkenndaten
- Bewertung des bestehenden Erstarrungsmodells
- Überprüfung der Auswirkung der periodischen Vorgänge und instationärer Zustände auf das Produkt (Spannungen und Verformungen in der Strangschale, Seigerungen)

Literaturverzeichnis

¹ Rauter, W.: Einfluss ausgewählter Gießparameter auf die Wärmeabfuhr in der Rundstranggießkokille. Diplomarbeit, Institut für Eisenhüttenkunde, Montanuniversität Leoben.

Castability of Steels: Influence of the Interfacial Properties on the Continuous Casting Process

A. Karasangabo and C. Bernhard

Interfacial phenomena play a very important role in the casting process of steel melts. Typical examples are the emulsification/entrainment of slag into the steel melt or vice versa at the slag/melt boundary, the collision and agglomeration of oxide inclusions in the steel melt, the entrapment of inclusions at the refractory interface, which can eventually lead to the clogging of the submerged entry nozzle, as well as the local corrosion of solid silica at the metal/slag interface as a result of the Marangoni convection. The present work presents a short review of the influence of interfacial properties on the continuous casting process. In the subsequent section, the Drop Shape Analysis unit, an apparatus for the measurement of interfacial properties at high temperatures based on the sessile drop method will be presented. A project at the "Christian Doppler Laboratory for Fundamentals of Metallurgy in Continuous Casting Processes" focuses on the influence of interfacial phenomena on SEN clogging.

Vergießbarkeit von Stählen: Einfluss von Grenzflächeneigenschaften auf den Stranggießprozess. Grenzflächeneigenschaften spielen im Stranggießprozess eine wichtige Rolle. Die Abscheidung nichtmetallischer Einschlüsse, die Keimbildung, das „Clogging“, die Erosion von Feuerfestmaterialien durch Marangonikonvektion, die Ausbildung des Meniskus und die Bildung von Oberflächenfehlern durch Gießschlackeneinziehung stehen in direktem Zusammenhang mit Grenzflächen- bzw. Oberflächenspannungen. Die Grundlagen und Hintergründe dieser Vorgänge werden im Überblick dargestellt. Der zweite Teil des Beitrags widmet sich einem Tropfenkonturanalysesystem, das die Messung von Benetzungswinkel und Oberflächenspannungen von Metall/Schlacke/Feuerfestsystemen bis 1650°C erlaubt. Im Rahmen eines Projekts am Christian-Doppler-Labor für „Metallurgische Grundlagen von Stranggießprozessen“ wird die Auswirkung von Grenzflächeneigenschaften auf das „Clogging“ untersucht werden.

1. Introduction

Interfacial phenomena play a very important role in the casting process of steel melts. Typical examples are the emulsification and entrainment of slag into the steel melt or vice versa at the slag/melt boundary, the collision and

agglomeration of oxide inclusions in the steel melt, the entrapment of inclusions at the refractory interface, which can eventually lead to the clogging of the submerged entry nozzle (SEN), as well as the local corrosion of solid silica at the metal/slag interface as a result of the Marangoni convection.

Furthermore, in the modelling of slag/metal systems, the knowledge of interfacial properties is indispensable in order to calculate similarity criteria between the modelling fluids and the real system. Since the literature data of surface/interfacial tension in liquid iron based alloys are scarce and largely scattered, there is a need to measure those properties on industrial steel melts and slags.

Dipl.-Ing. Augustin Karasangabo, Dipl.-Ing. Dr. mont. Christian Bernhard, Christian-Doppler-Labor für „Metallurgische Grundlagen von Stranggießprozessen“, Montanuniversität Leoben, Franz-Josef-Straße 18, A-8700 Leoben/Österreich. Vortrag gehalten bei der ersten wissenschaftlichen Evaluierung des CDL am 30. Oktober 2003.

The purpose of the present work is to present a short review of the influence of interfacial properties, particularly the contact angle and the surface tension on the continuous casting process, as treated in literature. In the subsequent section, an apparatus for the measurement of interfacial properties based upon the sessile drop method will be described.

2. Interfacial Properties in the Continuous Casting Process

The interfacial phenomena occurring during the continuous casting process can be divided into the factors affecting *the nucleation process, the removal of non-metallic inclusions (NMI), the nozzle clogging, the refractory erosion, surface defects, as well as the characterization of the meniscus in the mould*^{1,2,3}.

2.1 Nucleation Process

According to the classic nucleation theory, the degree of free energy of formation of a critical nucleus (energy barrier) during a heterogeneous nucleation depends largely on the interfacial tension between the solid phase (NMI, new metal crystal in liquid during solidification,...) and the melt as expressed by equation 1⁴, the contact angle being an index to evaluate the power of nucleation sites, which may be walls of a vessel, interface of different phases, etc.

$$\Delta G^* = \frac{16 \pi \gamma_{sl}^3 \cdot f(\theta)}{3 \Delta G_a^2}, \quad (\text{Eq. 1})$$

$$f(\theta) = \frac{1}{4}(2 - 3 \cos \theta + \cos 3\theta) \quad (\text{Eq. 2})$$

where ΔG^* is the energy barrier (Fig. 1⁵), γ_{sl} is the interfacial tension between solid and liquid phases, θ is the contact angle at the three-phase interface (Fig. 2), and ΔG_a is the activation energy to add one atom to the critical nucleus. Equation 1 and Figure 1 illustrate that nucleation must occur at a critical size (R^*) and that the energy barrier to nucleation can be reduced either by a decrease in interfacial tension γ_{sl} or by an increase in the volumetric driving force.

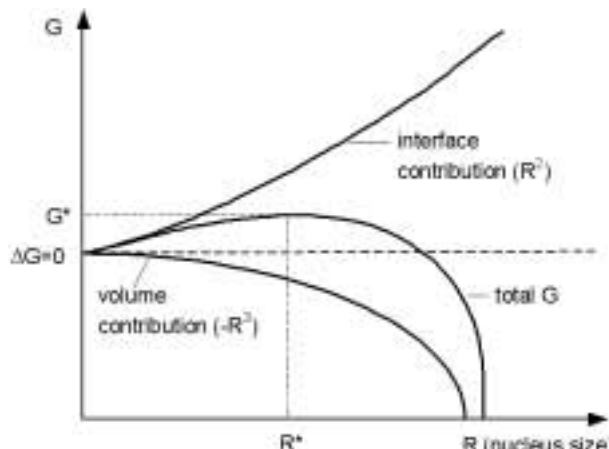


Fig. 1. Contribution of the interfacial tension to the total nucleation energy⁵

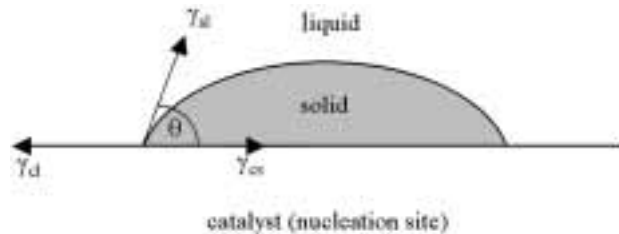


Fig. 2. Force balance at the three-phase interface

2.2 Removal of Inclusions from Molten Steel

In order to get removed from the steel melt, inclusions need to be transported and preferably dissolved into the slag phase or atmosphere¹. This process involves three steps: agglomeration, transport to the interface and separation across the interface. While the second step primarily involves fluid flow, the other two steps are strongly dependent upon interfacial properties^{1,6}.

2.2.1 Agglomeration of Non-Metallic Inclusions

Almost all solid inclusions are *not wetted* by liquid steel, i.e. $\theta > 90^\circ$ (Table 1^{7,8}) and thus will agglomerate due to capillary interaction if they come in contact with other similar solid inclusions or a refractory surface^{9,10,11}. Typical is the cluster formation of Al_2O_3 inclusions for which the contact angle with liquid iron is determined to be around 132° ^{12,13,14,15}. When two Al_2O_3 particles contact each other in the molten steel, a void (ΔP) is generated between them by the surface tension of the steel (σ_{Fe}) and the attraction force (F_A) works on the particles, as shown in Fig. 3¹⁶. In such a case, the balance of forces can be given by following equations^{2,10,11,16}:

$$\Delta P = \sigma_{Fe}(1/R_1 - 1/R_2) \quad (\text{Eq. 3})$$

$$F_A = 2\pi R_2 \sigma_{Fe}. \quad (\text{Eq. 4})$$

Tabelle 1. Analysenspannen des Stahlmarkenprogramms der Voestalpine Stahl Donawitz

C	0,02–1,2	%	Mo	0,01–1,1	%
Si	0,02–2,2	%	V	0,01–0,35	%
Mn	0,25–2,1	%	Sn	max. 0,01	%
P	0,01–0,1	%	B	0,0001–0,006	%
S	0,008–0,4	%	W	0,0001–0,6	%
Cr	0,05–2,5	%	As	max. 0,005	%
Ni	0,04–4,0	%	Nb	max. 0,02	%
Cu	0,03–0,6	%	Zr	max. 0,005	%
Al	0,002–0,07	%	O _{tot}	15–25	ppm
Ti	0,0015–0,12	%	H _{min}	1,3	ppm

The attraction force, which depends both on the contact angle (Fig. 4¹⁶) and the surface tension, is in the order of magnitude of 10^{-16} – 10^{-14} N, and becomes stronger with decreasing interparticle distance and increasing particle size^{10,16}.

In the injection metallurgy, the strong capillary attraction between solid alumina particles results in a quick collision, agglomeration, and formation of clusters at the three-phase interface on the surface of bubbles, when argon gas is injected into the molten steel bath^{11,17}.

2.2.2 Transport and Separation of NMI across the Interface

Flotation of inclusions

One factor which governs the inclusion removal from the bulk of a molten metal to a surface is the amount of

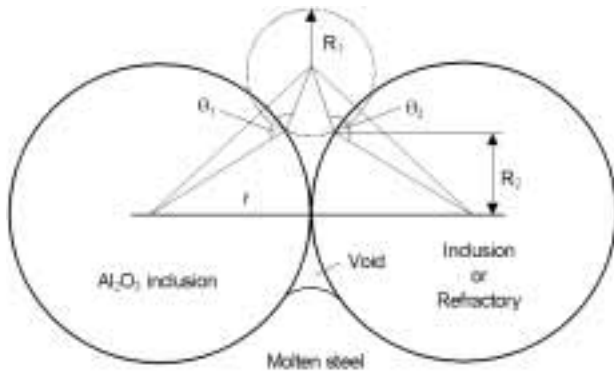


Fig. 3. Model of Al_2O_3 particle agglomeration due to surface tension of molten steel¹⁶

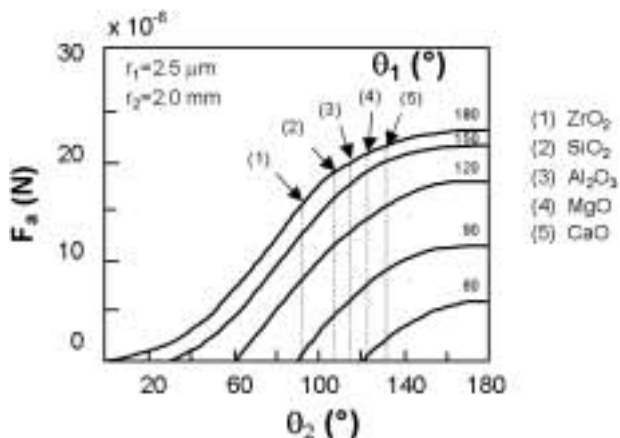


Fig. 4. Relation between contact angles and attraction force¹⁶

energy at the metal/solid interface. Flotation can only occur when the resultant change in free surface energy (ΔG) is less than zero, and the more negative the value of ΔG , the greater the probability for the inclusion to emerge and be retained at the interface. The condition for inclusion flotation is therefore^{6,7,18}:

$$\Delta G = \gamma_{ig} - \gamma_{mg} - \gamma_{mi} < 0, \quad (\text{Eq. 5})$$

where γ_{ig} and γ_{mg} are the surface tensions of the inclusion and the metal, respectively, and γ_{mi} stays for the interfacial tension between melt and inclusion. It follows that flotation would be facilitated by high values for γ_{mg} and γ_{mi} relative to γ_{ig} . However, irrespective of the value for γ_{mi} , the condition for flotation is satisfied when $\gamma_{ig} < \gamma_{mg}$ ^{6,13}. Consequently, the presence of even relatively low levels of any surface active element (S, O, ...) will lead to a marked diminution in the surface tension of the metal and thus give rise to a lower probability for stable flotation of inclusions^{6,19}. Equation 5 can be extended to the condition for a solid inclusion to float at a metal/slag interface¹⁸:

$$\Delta G = \gamma_{is} - \gamma_{ms} - \gamma_{mi} < 0, \quad (\text{Eq. 6})$$

i.e. flotation at a metal/slag interface would be most probable when $(\gamma_{ms} + \gamma_{mi}) > \gamma_{is}$, where γ_{is} = interfacial tension between inclusion and slag, γ_{ms} = interfacial tension between metal and slag, γ_{mi} = interfacial tension between metal and inclusion.

In industrial practice, bubble flotation is used to directly attach and entrap inclusions and hence lift them to the metal/tundish powder surface. Bubbling enhances

collision and agglomeration of inclusion particles by stirring the steel melt and promotes removal of agglomerated inclusion particles by flotation while the particles touch to bubbles. The fine Al_2O_3 -rich solid particles on argon bubble/steel melt interface can quickly agglomerate by the capillary attraction and form a large cluster. This explains why the removal of Al_2O_3 -rich solid inclusions by bubbling is more effective. Contrary, the fine liquid inclusion particles at argon bubble/steel melt interface do not demonstrate long-range attraction and agglomeration, and hence the growth of these inclusion particles by bubbling may be less pronounced¹¹.

Table 2. List of symbols and units

a:	capillary constant; height of the meniscus [m]
CC:	continuous casting
CCD:	charge-coupled device
F:	force [N]
g:	gravitational acceleration [m/s^2]
ΔG :	free energy of formation or reaction [J]
NMI:	nonmetallic inclusion
P:	pressure [Pa]
R:	radius of curvature [m]
SEN:	submerged entry nozzle
t_p :	residence time [s]
v_c :	casting speed [m/s]
Δ :	flotation coefficient [N/m]
γ_{xy} :	interfacial tension between x and y phases [N/m]
θ :	contact angle [°]
ρ :	density [kg/m^3]
σ_{xy} :	surface tension between x and y phases [N/m]

Subscripts:

g:	a quantity referring to the gas phase
i:	a quantity referring to an inclusion
l:	a quantity referring to the liquid phase
m:	a quantity referring to the metal (melt) phase
s:	a quantity referring to a slag phase

The bubble size is very important in the direct attachment and entrapment of inclusions, the efficiency increasing with decreasing bubble size. Bubbles with diameters between 1 and 10 mm can remove inclusions greater than 10 μm in diameter by direct entrapment¹⁸. The efficiency of inclusion removal increases with increasing inclusion size, flotation coefficient, surface tension of the metal and the contact angle^{1,20}. For good flotation it is necessary that the flotation coefficient (as defined in equation 7) should be positive and have a high value:

$$\Delta = \gamma_{mi} + \gamma_{mg} - \gamma_{ig} = \gamma_{mg}(1 - \cos\theta). \quad (\text{Eq. 7})$$

This is favoured when $(\gamma_{mg} + \gamma_{mi}) > \gamma_{ig}$, and also by non-wetting conditions ($\theta > 90^\circ$)¹⁸.

Filtration of steel melts

Ceramic filters can successfully remove inclusions as small as 1 μm from liquid steel, the filtration efficiency increasing with decreasing metal velocity, Reynolds number and bubble size as well as increasing inclusion size and density difference between inclusions and metal¹⁸.

Once inclusions are brought into contact with a filter, retention of the inclusions increases with increasing interfacial tension and with decreasing contact angle for liquid inclusions but increasing contact angle for solid inclusions^{16,18,21}.

2.3 Nozzle Clogging

One of the important tasks in steelmaking processes is to guarantee a good castability of the molten steel during the continuous casting process. The build-up of solid or

semisolid materials (principally Al_2O_3 , but also TiO_2 , ZrO_2 , etc.) on the SEN inner wall, also known as *nozzle clogging* represents a big obstacle to steel castability (Fig. 5²²) and has to be prevented.



Fig. 5. External view of clogged submerged entry nozzles²²

There are many different viewpoints concerning the source of particles that are deposited in a nozzle, thus leading eventually to its blockage. Some of the popular views are^{12,22-31}:

Deposition and agglomeration of indigenous NMI

This hypothesis is the most generally stated theory in literature²³⁻²⁹. According to it, the inclusions deposited at the nozzle orifice did not form *in-situ* but were already present in the bulk of the steel. They could originate from one or a combination of the following sources: deoxidation products from steelmaking and refining processes, reoxidation products from exposure of molten steel to air, slag entrapment, exogenous inclusions, chemical reactions such as products of inclusion modification. The problem is particularly severe in aluminium-killed steel grades, the adherence of the

alumina (Al_2O_3) inclusions to the nozzle refractory, and their subsequent sintering to form a network (Fig. 6¹²) being explained by the reduction in surface energy achieved^{24,27}.

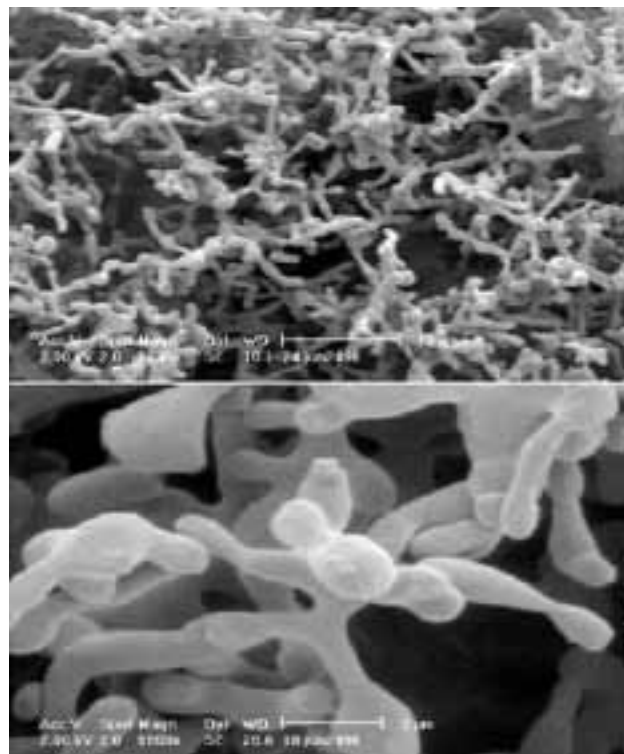


Fig. 6. High resolution SEM micrographs of Al_2O_3 inclusions after sintering to a network¹²

Reaction between liquid steel and the SEN refractory

When the molten steel flows through the SEN, dissolved aluminium in the steel can reduce solid or gaseous ox-

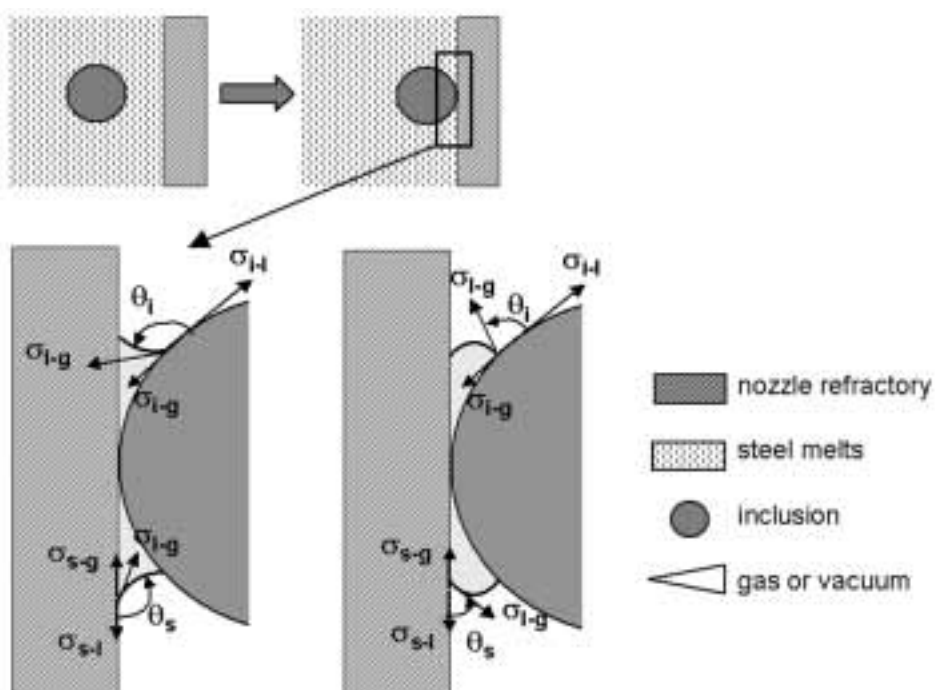


Fig. 7. Approach and adhesion of an inclusion to the surface of nozzle refractories³³

ides to form Al_2O_3 which is gradually deposited on the nozzle wall as the casting proceeds^{23,30,31}.

Precipitation of alumina on the refractory surface

This viewpoint suggests that the growth of the Al_2O_3 deposit is due to the precipitation of the dissolved aluminium and oxygen^{12,23,25}.

All of the phenomena listed above may possibly contribute to the blockage of the nozzle, the majority of work on SEN clogging suggests, however, that the main cause of that phenomenon is the poor wettability between the liquid steel and both NMI and oxides of the nozzle material^{9,32}. In short, it is the *high melting point* of some NMI, in combination with their *high surface tension* (poor or no wettability for liquid Fe) which is the core of the clogging problem^{24,26}.

The attachment of NMI on SEN refractories is achieved by three main steps strongly associated with interfacial phenomena which are the transport of the inclusions to the steel/refractory interface, the adhesion of the inclusions to the nozzle surface and the sintering of the inclusions with the nozzle refractories³³.

Figure 7³³ illustrates the attachment process of an inclusion to the surface of nozzle refractories exposed to steel melts. When an inclusion moves to the surface of nozzle refractories, it will either be pushed or attached depending on interfacial properties. In the second case, the steel melt withdraws between the nozzle refractory and the inclusion. Thus, a very small vacuum is produced between the surface of SEN refractories and the inclusion. At high temperatures ($>1400^\circ\text{C}$), the attached inclusions easily sinter to the SEN refractory and a firm adhesion occurs^{16,33}.

In metallurgical practice, making steel as clean as possible is the first step towards minimizing the SEN clogging. However, it is likely that clogging could still occur even if the steel was very clean. As research revealed, SEN blockage could happen if as little as one in every 1500 NMI were deposited on the nozzle wall²⁸. Thus, other ways to avoid that problem are being practiced. Those are^{24,34,35} the inclusion modification by calcium treatment, the flushing of argon gas through the nozzle, the coating of the inner bore of the SEN with

- poorly wettable materials to Al_2O_3 inclusions such as BN
- CaO-rich refractory so that Al_2O_3 inclusions will be converted to liquid calcium aluminates that will not adhere to the SEN
- C-free layer, in order to prevent the formation of oxides by reactions with C or CO (g) in the melt.

2.4 Marangoni Convection and Refractory Erosion

Erosion at the slag/gas or slag/metal interfaces, the so-called *slag line attack* is caused by the formation of Marangoni flows at the interfaces³⁶. For oxide materials (e.g. SiO_2) and systems where the dissolution of SiO_2 leads to an increase in surface tension, the region of the slag film in longer contact with the refractory will have higher SiO_2 contents. These regions will have higher surface tension values and a Marangoni flow will occur towards them^{9,36}.

As for the erosion of MgO/C and $\text{Al}_2\text{O}_3/\text{C}$ refractories, it occurs by a two stage process. When MgO particles protrude from the surface the refractory will be wetted by the slag (Fig. 8a) and the slag will dissolve the MgO , leaving carbon particles standing out from the surface. Under these conditions the metal phase will wet the refractory better than the slag (Fig. 8b). The metal there-

upon will dissolve the carbon leaving MgO protruding from the surface and the whole process will repeat^{9,36}.

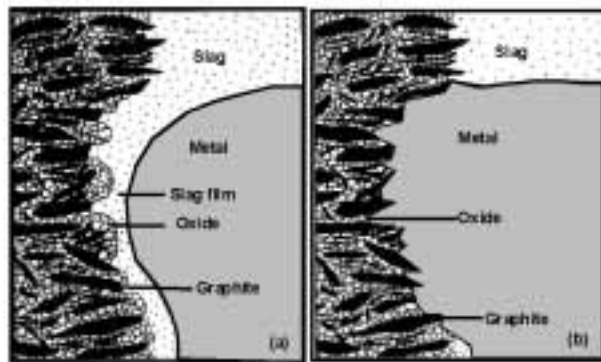


Fig. 8. Schematic representation of the manner in which local corrosion proceeds³³

2.5 Surface Defects during the CC Process

During the CC process various defects such as pinholes, blisters, slivers and pencil pipes arise through the entrapment of gas bubbles, slag, inclusions and mould flux on the newly solidified steel meniscus (Fig. 9³⁷). In the case of slag entrapment (Fig. 10¹), the detachment of slag is more likely to occur when the steel/slag interfacial tension (γ_{ms}) is low³⁸. Therefore, several mould powders have been formulated to provide high values of γ_{ms} . These usually involve the removal of Na_2O and any NaF from the flux. A decrease in the content of surface active elements is also an effective way of minimizing slag entrapment¹.

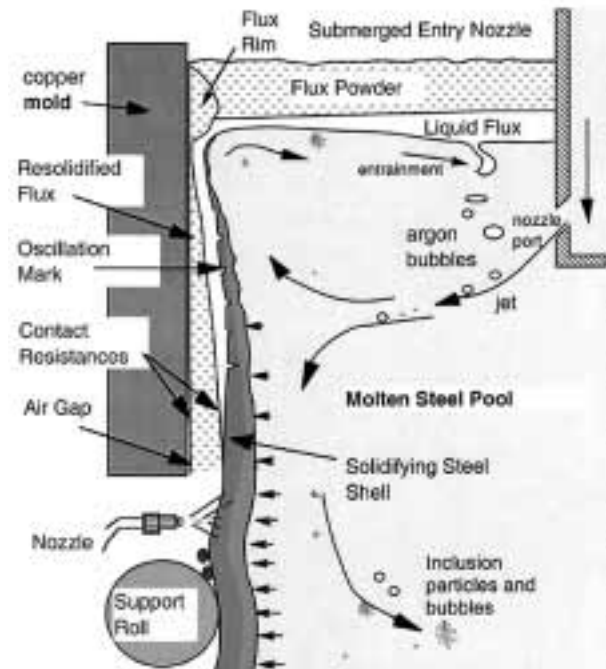


Fig. 9. Schematic of some phenomena contributing to the formation of surface defects³⁷

2.6 Meniscus Characterization

The metal level surface in the mould, the meniscus, is of vital importance for the surface quality of the cast product³⁹. The shape of the meniscus, which is determined by the capillary constant (a) as defined in

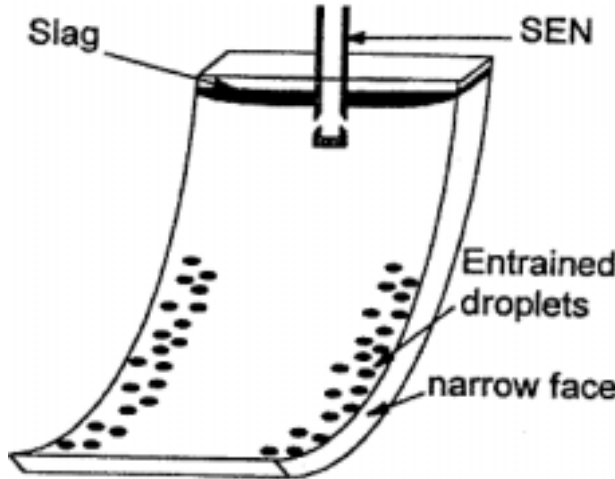


Fig. 10. Location of surface defects due to slag entrapment¹

equation 8, depends on the surface tension and the density of liquid iron, as well as on the contact angle between the mould and the melt^{40,41}:

$$a = \sqrt{\frac{2\sigma_{Fe}}{g \cdot \rho_{Fe}}} \quad (\text{Eq. 8})$$

Above equation shows that the greater the surface tension, the higher the meniscus, whose maximal height is given by $a/\sqrt{2}$, a value reached in the case of perfect non-wetting behaviour ($\theta = 180^\circ$) as it prevails between the mould wall and the steel melt⁴⁰.

The residence time of a certain quantity of liquid iron in the meniscus is expressed by:

$$t_R = a/v_c \quad (\text{Eq. 9})$$

The knowledge of t_R is very important for the prediction of the surface quality, a decrease in t_R contributes to the reduction of oscillation marks⁴⁰.

3. Measurement of Interfacial Properties

3.1 Experimental Method and Apparatus

Measurements of contact angles between solid substrates and liquids (steel melt, slags) are performed by the sessile drop method using a Drop Shape Analysis (DSA) apparatus, as shown in Fig. 11⁴².

The DSA apparatus consists of a tube furnace and a CCD camera with a light source. The working tube of the furnace is made of sintered Al_2O_3 with a molybdenum heating element. The heating rate of the sample changes with temperature at a rate of 15 K/min, the temperature inside the furnace being measured with a B-type thermocouple. The temperature is controlled by a PID digital programme regulator. Both ends of the reaction tube are sealed by watercooled caps.

The incorporated Windows software is used to process images of the drop acquired by the video camera and digitizing card of the DSA system. It offers the following possibilities: the measurement of the contact angle (θ), the measurement of the surface tension of the liquid (σ_l) and the calculation of the interfacial tension between solid and liquid phases (γ_{sl}).

The experimental procedure is as follows. Cylinders of samples weighing about 2–4 g are polished on faces

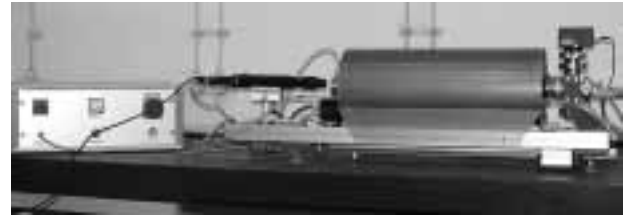


Fig. 11. The sessile drop unit – DSA – at the Institute of Ferrous Metallurgy in Leoben⁴²

with a grinder, then washed in acetone and dried before being placed on a ceramic substrate (Al_2O_3) which has to be washed with ethanol, dried and used without touching it to avoid any possible contamination. After the sample is placed at the center of the furnace, the system is sealed and flushed with argon gas before it is heated up to the experimental temperature of 1650°C in an argon gas atmosphere. Once the sample is melted, measurements of the contact angle and the surface tension are started. During the experiment, the shape of the sessile drop is monitored by a digital video camera. Selected images are stored either as bitmap (Fig. 12⁴²) or avi-file for future processing.

3.2 Outlook

Literature data about interfacial properties of iron alloys at high temperatures are very scattered, owing to the experimental difficulty of determining them accurately. Thus, an extensive experimental verification of the existing data with means of the DSA apparatus is scheduled. After the first measurements conducted on electrolytic iron, the next step is to measure the contact angle and the surface tension of iron containing various alloying and tramp elements as to determine their influence on interfacial properties and the castability of steel. Further, the effect of various gas atmospheres (argon, helium, reducing, ...) in the reaction chamber of the furnace on the interfacial properties will be investigated.

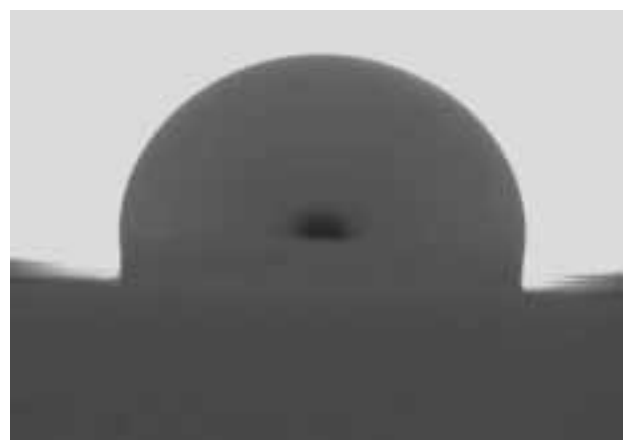


Fig. 12. A sessile drop of iron upon an Al_2O_3 substrate at 1580°C⁴² ($\theta = 128^\circ$)

It is also planned to use the thermochemical software *FactSage*⁴³ for the thermodynamic calculation of the interfacial tension between liquid iron alloys and molten slags under application of the *Good-Girifalco* relationship.

4. Summary

Interfacial phenomena play a very important role in the CC process of steel melts. The present paper has highlighted the influence of some of these phenomena in increasing or retarding the rates of chemical reactions during the CC process. In order to determine accurately the interfacial properties, an apparatus for the measurement of the contact angle and the surface tension of melts at high temperatures has been acquired by the Institute of Ferrous Metallurgy in Leoben.

At the Christian Doppler Laboratory for Fundamentals of Metallurgy in Continuous Casting Processes in Leoben, a project in cooperation with Voestalpine Stahl focusing on the issue of the influence of alloying elements on interfacial properties (surface tension, contact angle) of liquid steel and molten slags is underway. The knowledge of the role played by various alloying elements on interfacial properties of liquid steel should lead to a better control of the castability of some steel grades which are normally prone to SEN clogging.

References

- ¹ Mills, K. C., and S. Sridhar: Interfacial effects on iron and steelmaking processes. The Belton Memorial Symposium Proceedings, Sydney (2000), 211–226. – ² Emi, T., H. Shibata and H. Yin: Interfacial phenomena in refining and casting of steel melt. The Belton Memorial Symposium Proceedings, Sydney (2000), 195–207. – ³ Cramb, A. W., and I. Jimbo: Interfacial considerations in continuous casting, I&SM, 6 (1989), 43–55. – ⁴ Mizoguchi, S.: Structural control of casting. The Making, Shaping and Treating of Steel, 11th Edition: Casting Volume, The AISE Steel Foundation, Pittsburgh (2003), Chapter 11, 13–17. – ⁵ Kumari, M. R., P. S. Kumar and C. Subramanian: Effect of oxygen partial pressure on the nucleation kinetics of orthorhombic YBCO, Crystal Research and Technology, 37 (2002), 11, 1172–1179. – ⁶ Keene, B. J.: Surface tension of slag systems; Schlackenatlas, 2. Aufl., Verlag Stahleisen, Düsseldorf (1995), 403–462. – ⁷ Neifer, M., and P. Andrzejewski: Verbesserung des Reinheitsgrades in Stahlschmelzen durch Optimierung der Strömungsverhältnisse im Mehrphasensystem Schmelze/Gasblasen/Schlacke/Desoxidationsprodukte in Pfanne und Stranggießverteiler. Technische Forschung Stahl, Europäische Kommission, Luxemburg (1998). – ⁸ Kozakevitch, P., and L. D. Lucas: Revue de Métallurgie, 65 (1968), 589–598. – ⁹ Mukai, K.: Wetting and marangoni effect in iron and steelmaking processes. ISIJ International, 32 (1992), 1, 19–25. – ¹⁰ Sasai, K., and Y. Mizukami: Mechanism of alumina adhesion to continuous caster nozzle with Reoxidation of Molten Steel. ISIJ International, 41 (2001), 11, 1331–1339. – ¹¹ Yin, H., H. Shibata, T. Emi and M. Suzuki: In-situ observation of collision, agglomeration and cluster formation of alumina inclusion particles on steel melts. ISIJ International, 37 (1997), 10, 936–945. – ¹² Maddalena, R., R. Rastogi, B. El-Dasher and A. W. Cramb: Nozzle deposits in titanium treated stainless steels. ISS Electric Furnace Conference Proceedings, 58 (2000), 811–831. – ¹³ Nakashima, K., and K. Mori: Interfacial properties of liquid iron alloys and liquid slags relating to iron- and steelmaking processes. ISIJ International, 32 (1992), 1, 11–18. – ¹⁴ Cramb, A. W., and I. Jimbo: Surface tension values for use in casting. Turkdogan Symposium Proceedings, (1994), 196–206. – ¹⁵ Utigard, T.: Surface and interfacial tensions of iron based systems. ISIJ International, 34 (1994), 12, 951–959. – ¹⁶ Uemura, K., M. Takahashi, S. Koyama and M. Nitta: Filtration mechanism of non-metallic inclusions in steel by ceramic loop filter. ISIJ International, 32 (1992), 1, 150–156. – ¹⁷ Nogi, K., and K. Ogino: Role of interfacial phenomena in deoxidation process of molten iron. Canadian Metallurgical Quarterly, 22 (1983), 19–28. – ¹⁸ Hassal, G., and K. Mills: Fundamental studies related to the mechanisms of inclusion removal from steel. Technical Steel Research, European Communities, Luxembourg, (1998), 31–73. – ¹⁹ Lee, J., and K. Morita: Evaluation of surface tension and adsorption for liquid Fe-S alloys. ISIJ International, 42 (2002) 6, 588–594. – ²⁰ Keene, B. J.: Surface tension of slag systems, Schlackenatlas, 2. Aufl., Verlag Stahleisen, Düsseldorf (1995), 403–462. – ²¹ Janke, D., und K. Raiber: Grundlegende Untersuchungen zur Optimierung der Filtration von Stahlschmelzen. Technische Forschung Stahl, Europäische Kommission, Luxemburg (1996). – ²² Horbach, U., und H. Abratis: Untersuchung der Ursachen des Clogging in geregelten Ausgussystemen von Pfannen und Verteilern, insbesondere aus strömungstechnischer Sicht und unter Berücksichtigung der Druckverhältnisse. Technische Forschung Stahl, Europäische Kommission, Luxemburg (1997). – ²³ Thomas, B. G., and H. Bai: Tundish nozzle clogging – Application of computational models. ISS Steelmaking Conference Proceedings, 84 (2001), 895–912. – ²⁴ Rackers, K. G., and B. G. Thomas: Clogging in continuous casting nozzles. ISS Steelmaking Conference Proceedings, 78 (1995), 723–734. – ²⁵ Rastogi, R., and A. W. Cramb: Inclusion formation and agglomeration in aluminium-killed steels. ISS 84 Steelmaking Conference Proceedings, 84 (2001), 789–829. – ²⁶ Kemeny, F. L.: Tundish nozzle clogging – Measurement and prevention. Alex McLean Symposium Proceedings, Toronto, (1998), 103–110. – ²⁷ Wilson, F. G., M. J. Heesom, A. Nicholson and A. W. D. Hills.: Effect of fluid flow characteristics on nozzle blockage in aluminium-killed steels. Ironmaking and Steelmaking, 14 (1987), 1, 296–309. – ²⁸ Dawson, S.: Tundish nozzle blockage during the continuous casting of aluminium-killed steel. I&SM, 4 (1990), 33–42. – ²⁹ Singh, S. N.: Mechanism of alumina build-up in tundish nozzles during continuous casting of aluminium-killed steels. Metallurgical Transactions B, 5 (1974), 2165–2178. – ³⁰ Poirier, J., B. Thillou, M. A. Guibon and G. Provost: Mechanisms and countermeasures of alumina clogging in submerged nozzles. ISS Steelmaking Conference Proceedings, 78 (1995), 451–456. – ³¹ Gao, Y., and K. Sorimachi: Formation of clogging materials in an immersed nozzle during continuous casting of titanium stabilized stainless steel. ISIJ International, 33 (1993), 2, 291–197. – ³² Kim, D. S., H. S. Song, Y. D. Lee, Y. Chung and A. W. Cramb: Clogging of the submerged entry nozzle during the casting of titanium bearing stainless steels. ISS Steelmaking Conference Proceedings, 80 (1997), 145–152. – ³³ Valentini, P., A. Heinen, S. Landa, D. Janke and Z. Ma: Improvement of cleanliness and grain size in Ca-treated and Al-deoxidized steels with high S-contents in billet and bloom casting. Technical Steel Research, European Commission, Brussels, 7 (1999), 27–36. – ³⁴ Bannenberg, N.: Inclusion modification to prevent nozzle clogging. ISS Steelmaking Conference Proceedings, 78 (1995), 457–463. – ³⁵ Höller, W.: Verringerung der Ansatzbildung bei Tauchrohren für das Stranggießen von Stahl durch Einbringen einer kohlenstofffreien Innenschicht. Veitsch-Radex Rundschau, 1 (1999), 30–39. – ³⁶ Mukai, K.: Marangoni flow and corrosion of refractory walls. Philosophical Transactions of the Royal Society, London, 356 (1998), 1015–1026. – ³⁷ Thomas, B. G.: Modelling of continuous casting. The Making, Shaping and Treating of Steel, 11th Edition: Casting Volume, The AISE Steel Foundation, Pittsburgh (2003), Chapter 5. – ³⁸ Cramb, A. W.: Proceedings of the 5th International Conference on Molten Slags, Fluxes and Salts, Sydney (1997), 35–50. – ³⁹ Toshihiro, E.: Surface defects on continuously cast strands. The Making, Shaping and Treating of Steel, 11th Edition: Casting Volume, The AISE Steel Foundation, Pittsburgh (2003), Chapter 21. – ⁴⁰ Ackermann, P.: Processus de formation de marques de surface, typique de la coulée en lingotière fortement refroidie. Thèse N° 503, EPFL, Lausanne (1983), 20–32. – ⁴¹ Hampe, M. J.: Interface Science, Link: <http://www.tu-darmstadt.de/fb/mb/tvt/neu/tvt-Dateien/lehre/skripte/gvtohp04.pdf>. – ⁴² Karasangabo, A.: DSA Measurements, Leoben, (2003). – ⁴³ GTT Technologies and Termfact & Ecole Polytechnique CRCT: FactSage™, website: <http://www.factsage.com/>.